IPP-Report

Max-Planck-Institut für Plasmaphysik

E. Harmeyer, J. Kisslinger, H. Wobig

The Effect of Ferritic Structural Material on the Magnetic Field of Stellarators

IPP III/241

Mai 1999

The Effect of Ferritic Structural Material on the Magnetic Field of Stellarators

E. Harmeyer, J. Kisslinger, H. Wobig

Abstract:

In a fusion reactor ferritic steel is strongly favoured as structural material, since the low activation after neutron irradiation makes it a very attractive candidate to mitigate the issue of radioactive waste disposal. On the other side ferromagnetic material modifies the magnetic field of the current carrying coils and may have negative effects on the plasma confinement. Especially in stellarators any deviation from symmetry may lead to island formation and destruction of magnetic surfaces. In the following paper the general equations governing the magnetic field in stellarators with ferritic structural material are analysed and the basic effects are investigated in simple straight geometry where analytic solutions are available. A code has been established which allows one to compute the modified field in toroidal geometry. Since the ferritic material is saturated under reactor conditions, the effective permeability is in the range of 1.2 to 1.5. This leads to a small reduction of the rotational transform under normal conditions in which the symmetry of the field generated by the coils is not violated.
Symmetry breaking error fields arise if the properties of the ferritic matter differ from period to period. This case has been simulated by the assumption of inhomogeneous magnetization in the 5 blanket modules. In is found that the islands in the boundary region, which in a Helias reactor are utilized for divertor actions can be strongly modified by these error fields, thus care must be taken to avoid geometrical and material asymmetries of a Helias reactor.

1. Introduction

Magnetic surfaces of stellarator configurations are sensitive to field perturbations which may create islands on rational surfaces or destroy the last magnetic surface. In judging the importance of error fields two cases have to be distinguished: symmetry-breaking perturbations and perturbations which maintain the symmetry of the unperturbed configuration. If the error field has another toroidal periodicity as the unperturbed field, islands will arise on resonant magnetic surfaces. These perturbations are the result of misalignment of the coils or manufacturing errors of the coils. In order to keep this effect below a tolerable level the relative error field should be kept below 10^{-4}. If the error field preserves the symmetry of the unperturbed case resonant effects do not occur, however, the magnetic surfaces will be modified and the rotational transform will be changed. This modification happens if the plasma pressure grows and the plasma currents introduce a symmetry-preserving field $\boldsymbol{B}_1$, which, together with the magnetic field $\boldsymbol{B}_0$ of the coils, provides the self-consistant equilibrium field $\boldsymbol{B}$. The difference between the finite beta-field and the vacuum field is a function of beta and it may reach 5% or more. In a Helias configuration this effect causes the last magnetic surface to shrink and it slightly modifies the rotational transform.

A further modification of the magnetic field in stellarators will be provided by ferritic material in blanket and shield of a fusion reactor. These ferritic/martensitic steels are favoured as structural material because of the low long-term activation[1]. The magnetic field of the coils is modified by ferritic steel although the steel will be in saturation and the effective permeability will be close to unity. Properties of ferritic steel have been investigated in Karlsruhe (FZK)[2].

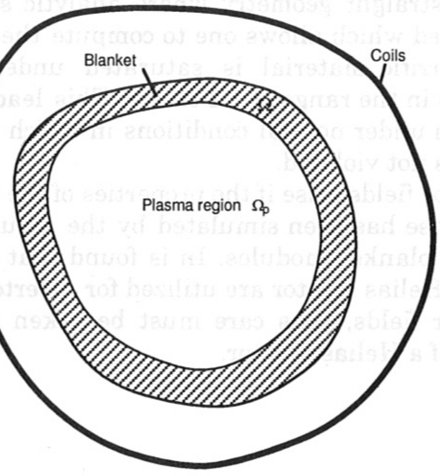

Fig 1: Scheme of modular coils and blanket in a Helias fusion reactor. In the following computations the blanket will be replaced by a homogeneous layer with an effective constant permeability.

---

[1] A. Koyama, A. Hishnuma, D.S. Gelles, R.L. Klueh, W. Dietz, K. Ehrlich, J. of Nucl. Materials 233 - 237 (1996) 138 - 147

[2] K. Ehrlich, D.R. Harries, A. Möslang, Characterisation and Assessment of Ferritic/Martensitic Steels, Wissenschaftliche Berichte FZKA 5626, Feb. 1997

In a strong magnetic field the ferritic steel is saturated leading to a fixed magnetization along the direction of the magnetic field $\boldsymbol{H}$. In case of Manet this magnetization is 1.6 T, in another material F82H it is even higher[3]. Let be M the magnetization in saturation, then we may write

$$\boldsymbol{M} = M\frac{\boldsymbol{H}}{H}$$

Thus, the susceptibility of the material is a function of H. The task remains to compute the magnetic field self-consistantly taking into account the continuity conditions of B_n at the boundaries of the ferritic material.

2. Basic Equations

As indicated in the introduction the following ansatz can be made if the material is saturated

$$\mu = \mu_0\left(1 + \frac{M}{H}\right) = \mu(H) \tag{1}$$

M is the saturated magnetization. Inside the domain Ω the equation of the magnetic field is

$$\nabla\bullet\mu\boldsymbol{H} = 0 \Rightarrow \mu\nabla\bullet\boldsymbol{H} + \boldsymbol{H}\bullet\nabla\mu = 0 \tag{2}$$

The ansatz

$$\boldsymbol{H} = \boldsymbol{H}_0 + \nabla\Phi \tag{3}$$

leads to

$$\Delta\Phi = -\boldsymbol{H}\bullet\nabla\, ln\,(\mu) \tag{4}$$

$\boldsymbol{H}_0$ is the vacuum field of the coil system. The boundary conditions require that

$$\mu\left(\boldsymbol{H}_0 + \nabla\Phi\right)\bullet\boldsymbol{n} \tag{5}$$

be continuous across the boundary of Ω. The solution of eq. 4 is

$$\Phi = \frac{1}{4\pi}\iiint_\Omega \frac{\boldsymbol{H}\bullet\nabla\, ln\,(\mu)}{|\boldsymbol{x}-\boldsymbol{y}|}d^3\boldsymbol{y} + \iint_S \frac{\sigma(\boldsymbol{y})}{|\boldsymbol{x}-\boldsymbol{y}|}d^2\boldsymbol{y} \tag{6}$$

The second term is needed to satisfy the boundary condition (5). The normal derivative of

$$\Phi_1 = \frac{1}{4\pi}\iiint_\Omega \frac{\boldsymbol{H}\bullet\nabla\, ln\,(\mu)}{|\boldsymbol{x}-\boldsymbol{y}|}d^3\boldsymbol{y} \tag{7}$$

---

[3] P. Ruatto, Wissenschaftliche Berichte FZKA 5683, 1996

is continuous across the boundary[4].

$$\left.\frac{\partial \Phi_1}{\partial n}\right|_i = \left.\frac{\partial \Phi_1}{\partial n}\right|_a \tag{8}$$

The normal derivative of the second term is discontinuous and the relation holds

$$\frac{\partial \Phi_2}{\partial n} = \iint_S \sigma(y) \frac{\partial}{\partial n} \frac{1}{|x-y|} d^2y \pm 2\pi\sigma(x) \tag{9}$$

The plus sign holds for the limit from the inner side and the minus sign for the outer limit. In eq. (9) **x** is a point on the boundary. Using the abbreviation

$$K\sigma = \iint_S \sigma(y) \frac{\partial}{\partial n} \frac{1}{|x-y|} d^2y \tag{10}$$

the boundary condition (5) yields the integral equation

$$(\mu - 1)K\sigma + (\mu + 1)2\pi\sigma = -(\mu - 1)H_{0,n} - \mu \left.\frac{\partial \Phi_1}{\partial n}\right|_i + \left.\frac{\partial \Phi_1}{\partial n}\right|_a \tag{11}$$

From eq. 6 and 3 we get

$$\boldsymbol{H} = \boldsymbol{H}_0 + \nabla \frac{1}{4\pi} \iiint_\Omega \frac{\boldsymbol{H} \bullet \nabla \ln(\mu)}{|\boldsymbol{x}-\boldsymbol{y}|} d^3y + \nabla \iint_S \frac{\sigma(y)}{|\boldsymbol{x}-\boldsymbol{y}|} d^2y \tag{12}$$

Since the domain of the blanket is multi-connected, the second surface integral has to be taken over all surfaces of the blanket. The two integral equations (11) and (12) can be solved iteratively. In lowest order the right side is computed inserting the vacuum field $\boldsymbol{H}_0$. The numerator of the first integral is

$$\boldsymbol{H} \bullet \nabla \ln(\mu) = -\frac{M}{H+M} \boldsymbol{H} \bullet \frac{\nabla H}{H} \tag{13}$$

The volume integral is written as

$$\boldsymbol{H}_1 = \nabla \frac{1}{4\pi} \iiint_\Omega \frac{\boldsymbol{H} \bullet \nabla \ln(\mu)}{|\boldsymbol{x}-\boldsymbol{y}|} d^3y = \frac{1}{4\pi} \iiint_\Omega \frac{M}{H+M} \boldsymbol{H} \bullet \frac{\nabla H}{H} \frac{\boldsymbol{x}-\boldsymbol{y}}{|\boldsymbol{x}-\boldsymbol{y}|^3} d^3y \tag{14}$$

and the field of the coils

[4] Smirnov, Lehrbuch der Höheren Mathematik, Bd. II

$$H_0 = \frac{1}{4\pi} \iiint_{Coils} \frac{j \times (x-y)}{|x-y|^3} d^3y \tag{15}$$

j is the current density in the coils. A rough estimate of the field (14) can be made by

$$|H_1| \leq \frac{H_{max} |\nabla \ln \mu|_{max}}{4\pi} \iiint_\Omega \frac{1}{|x-y|^2} d^3y \tag{16}$$

with

$$|\nabla \ln \mu|_{max} = \frac{M}{(H_{min}+M)} \left|\frac{\nabla H}{H}\right|_{max} \tag{17}$$

3. Homogeneous Blanket.

Because of the inhomogeneity of μ the perturbation field consists of two terms given in eq. 12. In the following we approximate the permeability μ by its maximum value and consider this as a constant throughout the blanket region. This approximation also applies to an experimental device where structural material with a finite permeability is used. Let us denote the inner and outer boundaries of the blanket with S_1 and S_2 .The boundary condition yield on S_1

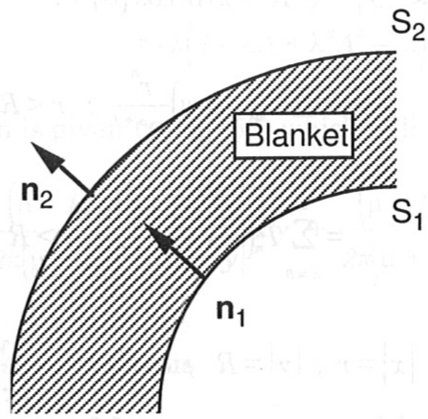

Fig. 2: Scheme of blanket.

The boundary conditions on S_2 are

$$\mu\left(H_0 \bullet n_2 + \frac{\partial \Phi_2}{\partial n}\right)\Big|_i = \left(H_0 \bullet n_2 + \frac{\partial \Phi_2}{\partial n}\right)\Big|_a \tag{18}$$

and on the inner surfaces S_1

$$\left(H_0 \bullet n_1 + \frac{\partial \Phi_2}{\partial n}\right)\Big|_i = \mu\left(H_0 \bullet n_1 + \frac{\partial \Phi_2}{\partial n}\right)\Big|_a \tag{19}$$

Using the relation (9) we get two integral equations for the „charge" σ_1 and σ_2.
On S_2

$$(\mu-1)K_2\sigma_2+(\mu+1)2\pi\sigma_2+(\mu-1)K_1\sigma_1=-(\mu-1)H_{0,n2} \tag{20}$$

and

$$-(\mu-1)K_1\sigma_1+(\mu+1)2\pi\sigma_1-(\mu-1)K_2\sigma_2=(\mu-1)H_{0,n1} \tag{21}$$

on S_1.
Here we have used the notation

$$K_1\sigma_1=\iint_{S1}\sigma_1(y)\frac{\partial}{\partial n}\frac{1}{|\boldsymbol{x}-\boldsymbol{y}|}d^2\boldsymbol{y} \tag{22}$$

These are two coupled integral equations. In the limit μ --> 1 the magnetic field of the coils is unchanged. The function

$$\frac{1}{|\boldsymbol{x}-\boldsymbol{y}|}$$

is the Green's function of the Laplace operator. The Green's function can be expanded in terms of eigenfunction of the Laplace operator. Another expansion is provided by Legendre functions.

$$\frac{1}{|\boldsymbol{x}-\boldsymbol{y}|}=\frac{1}{\sqrt{R^2-2Rr\cos(\psi)+r^2}}$$

$$=\sum_{n=0}^{\infty}P_n(\cos\psi)\frac{r^n}{R^{n+1}}\ ;\quad r<R$$

$$=\sum_{n=0}^{\infty}P_n(\cos\psi)\frac{R^n}{r^{n+1}}\ ;\quad r>R \tag{23}$$

with

$$|x|=r\ ;\ |y|=R\ ;\ \cos(\psi)=\frac{\boldsymbol{x}\bullet\boldsymbol{y}}{|y||x|}$$

on S_2. This expansion is widely used in computing the distortion of a magnetic field in spherical geometry. The integral equations can be solved by an iterative procedure. For this purpose we introduce the vectors

$$\sigma=\begin{pmatrix}\sigma_1\\ \sigma_2\end{pmatrix}\ ;\ h_n=\begin{pmatrix}H_{0,n}(S_1)\\ -H_{0,n}(S_2)\end{pmatrix} \tag{24}$$

and the integral operators

$$K\sigma=\begin{pmatrix}-K_1\sigma_1\\ K_2\sigma_2\end{pmatrix}\ ;\ M\sigma=\begin{pmatrix}-K_2\sigma_2\\ K_1\sigma_1\end{pmatrix} \tag{25}$$

The system of equations can be written as

$$(\mu - 1)K\sigma + (\mu + 1)2\pi\sigma + (\mu - 1)M\sigma = -(\mu - 1)h_n \tag{26}$$

and the iterative procedure yields

$$(\mu - 1)K\sigma_{k-1} + (\mu + 1)2\pi\sigma_k + (\mu - 1)M\sigma_{k-1} = -(\mu - 1)h_n \tag{27}$$

The lowest order solution is

$$(\mu + 1)2\pi\sigma_k = -(\mu - 1)h_n \tag{28}$$

Definitions:

$$\lambda = \frac{(\mu - 1)}{(\mu + 1)2\pi} \quad ; \; A\sigma = K\sigma + M\sigma \tag{29}$$

The system is in short notation

$$\lambda A\sigma + \sigma = -\lambda h_n \tag{30}$$

and the solution in a Neumann series is

$$\begin{aligned}\sigma &= -\lambda(1 + \lambda A)^{-1} h_n \\ &= -\lambda\left(1 - \lambda A + \lambda^2 A^2 - \ldots\right)h_n\end{aligned} \tag{31}$$

On lowest order the solution is given by eq. (39) which will be inserted into eq. 2

$$\Phi = -\frac{(\mu - 1)}{2\pi(\mu + 1)}\iint_{S1}\frac{H_{0,n}(y)}{|x-y|}d^2y + \frac{(\mu - 1)}{2\pi(\mu + 1)}\iint_{S2}\frac{H_{0,n}(y)}{|x-y|}d^2y \tag{32}$$

The magnetic field in the plasma region is

$$\boldsymbol{H} = \boldsymbol{H}_0 + \iint_{S1}\frac{\sigma_1(y)(x-y)}{|x-y|^3}d^2y + \iint_{S2}\frac{\sigma_2(y)(x-y)}{|x-y|^3}d^2y \tag{33}$$

which in lowest order is

$$\boldsymbol{H} = \boldsymbol{H}_0 - \frac{(\mu - 1)}{2\pi(\mu + 1)}\left\{\iint_{S1}\frac{H_{0,n}(y)(x-y)}{|x-y|^3}d^2y - \iint_{S2}\frac{H_{0,n}(y)(x-y)}{|x-y|^3}d^2y\right\} \tag{34}$$

The electrostatic equivalent to this equation is the electric field of a surface charge

$$\frac{2(\mu - 1)}{(\mu + 1)} H_{0,n}(y) \tag{35}$$

This effective „surface charge" changes sign on the surface and it produces a dipole field in lowest order. The blanket in a Helias reactor has a helical shape, which is aligned to the helical shape of the magnetic surfaces. For this reason the toroidal component of the vacuum field has a normal component on the boundary of the blanket which will lead to an $l = 1$ type perturbation field in the plasma region. The elliptical shape of the geometry introduces another $l = 2$ type perturbation field.

3.1 Straight $l = 2$ - Stellarator.

In a straight stellarator the helical windings are wound onto a vacuum tube which is cylindrical and has a permeability μ. The geometry is sketched in Fig. 3. We employ a cylindrical coordinate system r,φ,z. Because of the helical invariance the magnetic field is only a function of r and φ - kz.

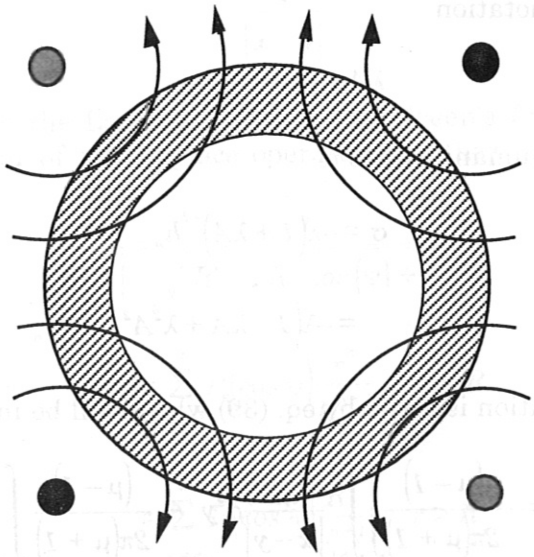

Fig. 3: Scheme of a straight l=2-stellarator.

The paramagnetic ring will reduce the poloidal field of the helical winding and hence reduce the rotational transform in the inner region. The homogeneous z-field is not changed by the ring since the boundary is parallel to the z-field.

The magnetic potential is

$$\Phi_a = B_a z + \frac{1}{k}\left(aI_2(2kr) + bK_2(2kr)\right) \sin(2\varphi) \tag{36}$$

in the ring

$$\Phi_R = B_R z + \frac{1}{k}\left(cI_2(2kr) + dK_2(2kr)\right) \sin(2\varphi) \quad (37)$$

and in the inner region

$$\Phi_i = B_i z + \frac{1}{k} eI_2(2kr) \sin(2\varphi) \quad (38)$$

The phase φ is given by θ-kz. θ is the poloidal angle. The boundary conditions yield (with $x = 2kr$)

$$B_i = B_a \ ; \ \mu B_a = B_R \quad (39)$$

$$eI_2'(x_1) = cI_2'(x_1) + dK_2'(x_1) \quad (40)$$

$$\mu eI_2(x_1) = cI_2(x_1) + dK_2(x_1) \quad (41)$$

$$aI_2'(x_2) + bK_2'(x_2) = cI_2'(x_2) + dK_2'(x_2) \quad (42)$$

$$\mu aI_2(x_1) + \mu bK_2(x_1) = cI_2(x_1) + dK_2(x_1) \quad (43)$$

This yields the relations

$$D(x) = I_2'(x)K_2(x) - I_2(x)K_2'(x) \quad (44)$$

$$D(x_1)c = e\left(I_2'(x_1)K_2(x_1) - \mu I_2(x_1)K_2'(x_1)\right) \quad (45)$$

$$D(x_1)d = e(\mu - 1)I_2'(x_1)I_2(x_1) \quad (46)$$

$$\mu aD(x_2) = c\left(\mu I_2'(x_2)K_2(x_2) - I_2(x_2)K_2'(x_2)\right) + d(\mu - 1)K_2(x_2)K_2'(x_2)$$

$$\mu aD(x_2) = c\left(\mu I_2'(x_2)K_2(x_2) - I_2(x_2)K_2'(x_2)\right) + d(\mu - 1)K_2(x_2)K_2'(x_2) \quad (47)$$

Inserting (28) and (29) into (30) yields a relation between *e* and *a*. In case μ --> 1 we find *a* = *e*. In general the field is reduced by a factor (*e* = *a* factor1). factor1 is the reduction factor of the external helical field due to the paramagnetic ring.

Numerical example:
x_1=2kr = 1.136, x_2= 2kr = 1.59. In a Helias reactor (R = 22 m, 5 periods, k=5/R) this yields r_1 = 2.5 m and r_2 = 3.43 m. The width of the paramagnetic shell is 0.93 m.

Table 2

μ	x_1	x_2	factor1	factor2
1	1.136	1.59	1	1
1.03	1.136	1.59	1.0001	0.9998
1.06	1.136	1.59	0.9999	0.9993
1.09	1.136	1.59	0.9993	0.9986
1.12	1.136	1.59	0.9985	0.9976
1.15	1.136	1.59	0.9975	0.9963
1.18	1.136	1.59	0.9961	0.9949
1.21	1.136	1.59	0.9946	0.9933
1.24	1.136	1.59	0.9929	0.9914
1.27	1.136	1.59	0.9910	0.9895
1.3	1.136	1.59	0.9889	0.9873
1.33	1.136	1.59	0.9866	0.9850

The second factor2 has been computed in straight geometry neglecting the helicity of the $l = 2$-windings. The result shows that the reduction of the poloidal field is less than 1%, this implies that the reduction of the rotational transform is less than 2%.

3.2 Modular Ripple

A further case, which can be examined analytically, is the reduction of the modular ripple by a ferritic shell. We consider a coil system of circular coils, which are aligned along the z-axis and may be considered as an approximation to the modular coils of a Helias reactor. Outside the ring the magnetic potential is

$$\Phi_a = B_a z + \frac{1}{k}\left(aI_0(kr) + bK_0(kr)\right) sin(kz) \tag{48}$$

inside the ring

$$\Phi_R = B_R z + \frac{1}{k}\left(cI_0(kr) + dK_0(kr)\right) sin(kz) \tag{49}$$

and in the inner region

$$\Phi_i = B_i z + \frac{1}{k}\, eI_0(kr)\, sin(kz) \tag{50}$$

The components of the magnetic field are

$$B_r^R = \left(cI_0'(kr) + dK_0'(kr)\right) sin(kz)$$

$$B_r^a = \left(aI_0'(kr) + bK_0'(kr)\right) sin(kz)$$

$$B_r^i = eI_0'(kr)\, sin(kz) \tag{51}$$

The continuity of the radial components yields the boundary conditions

$$eI_0'(x_1) = cI_0'(x_1) + dK_0'(x_1) \tag{52}$$

$$aI_0'(x_2) + bK_0'(x_2) = cI_0'(x_2) + dK_0'(x_2)$$

The z-components of the magnetic field are

$$B_z^a = B_a + \left(aI_0(kr) + bK_0(kr)\right) cos(kz) \quad B_z^R = B_R + \left(cI_0(kr) + dK_0(kr)\right) cos(kz)$$

$$B_z^i = B_i + eI_0(kr)\, cos(kz) \tag{53}$$

From which the boundary conditions are obtained

$$\mu eI_0(x_1) = cI_0(x_1) + dK_0(x_1)$$

$$\mu \left(aI_0(x_2) + bK_0(x_2)\right) = cI_0(x_2) + dK_0(x_2) \tag{54}$$

The boundary conditions (35) and (37) determine the coefficients *e,c* and *d* as functions of *a*. The structure of these boundary conditions is the same as in eqs. (23) - (26). The results

$$D(x) = I_0'(x)K_0(x) - I_0(x)K_0'(x) = \frac{1}{x}$$

$$D(x_1)c = e\left(I_0'(x_1)K_0(x_1) - \mu I_0(x_1)K_0'(x_1)\right)$$

$$D(x_1)d = e(\mu - 1)I_0'(x_1)I_0(x_1)$$

$$\mu a D(x_2) = c\left(\mu I_0'(x_2)K_0(x_2) - I_2(x_0)K_0'(x_2)\right) + d(\mu - 1)K_0(x_2)K_0'(x_2) \tag{55}$$

Introducing some definitions

$$A = \left(\mu I_0'(x_2)K_0(x_2) - I_2(x_2)K_0'(x_2)\right), \quad C = \left(I_0'(x_1)K_0(x_1) - \mu I_0(x_1)K_0'(x_1)\right)$$

$$E = I_0'(x_1)I_0(x_1)K_0(x_2)K_0'(x_2) \tag{56}$$

allows one to write the reduction of the ripple in shorter form

$$e = a\,\frac{\mu D(x_2)D(x_1)}{AC + (\mu - 1)^2 E} \tag{57}$$

The result is the reduction factor e/a in terms of Bessel functions.

4. Toroidal Geometry

In toroidal geometry analytic results are not available and numerical computations are needed to find the modification of the magnetic field. For this reason a numerical program has been developed with solves the integral equations described in chapter 2. To compare the results with analytic estimates a toroidal l = 2 stellarator has been computed. The same geometry as described in Fig. 3 has been selected in toroidal geometry. The data listed in table 2 have been extended to a μ-value of 5 and have been compared with numerical results. The permeability is constant in the blanket region. The difference between the results of the straight stellarator and its toroidal equivalent are expected to be in the order of the inverse aspect ratio.
The rotational transform of a straight helical l = 2 - stellarator scales with the square of the factor e in equation (38). Fig. 4 shows a good coincidence between the analytical results of the straight helical stellarator and the numerical results of the toroidal case. The increase of the permeability from μ = 1 to μ = 2 leads to a decrease of the rotational transform of about 20%.

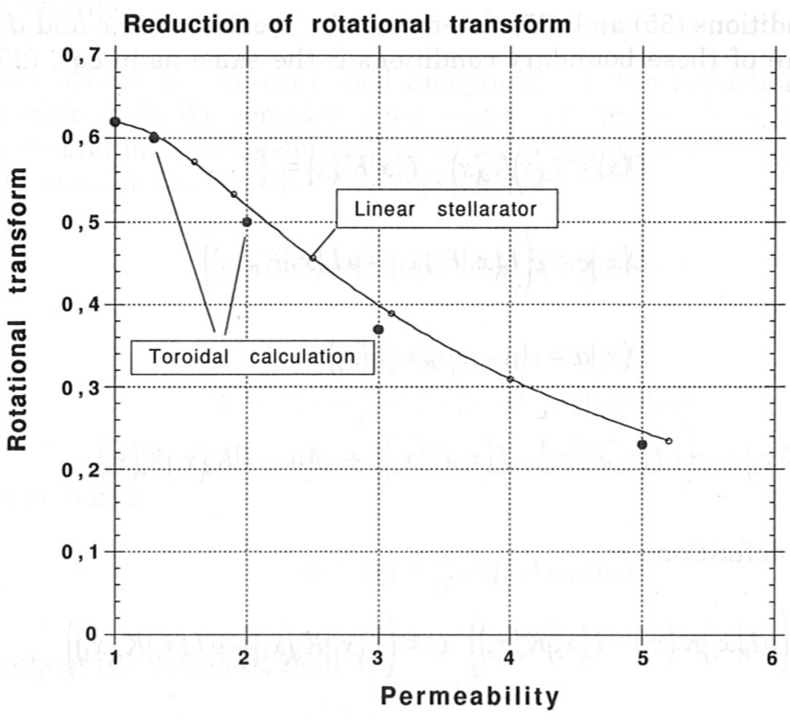

Fig. 4: Comparison of the rotational transform in an l = 2 stellarator between straight and toroidal geometry. The transform is reduced due to the screening effect of the paramagnetic shell. The dots are the results of numerical calculations in toroidal geometry, which show sufficient coincidence with the result of analytic theory.

5. Helias Reactor

The magnetic field of a Helias reactor is generated by a set of modular coils and the magnetic surfaces are quite different from those of a classical $l = 2$ stellarator. However, as shown in the example above, it is expected that the rotational transform is reduced by the presence of ferritic material in blanket and shield. Furthermore, any asymmetry of the structural components, either caused by geometric misalignments or by inhomogeneities of the ferritic material, may lead to error fields which cause island formation as it is well known from misalignment of the modular coils.

The following figure displays a section of blanket and shield of a Helias reactor. The goemetry of the blanket modules and the shielding components is rather complex, for this reason a simplified model is adopted where a homogeneous of constant width surrounds the plasma. In the computation the difference between breeding blanket and shield is not existent.

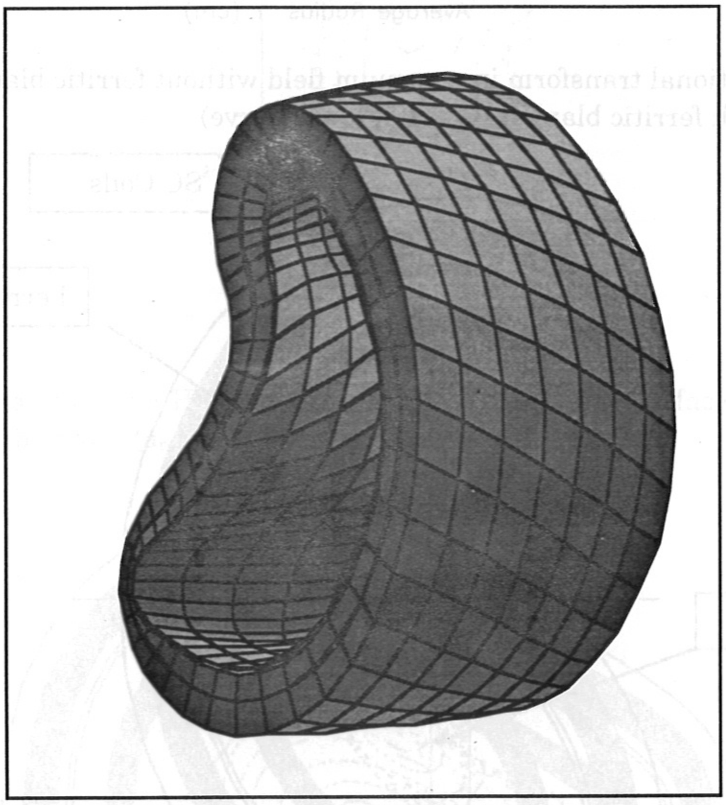

Fig. 5: Part of blanket and shield in a Helias reactor

The first case, which will be investigated in the following, is a homogeneous blanket, which does not destroy the 5-fold symmetry of the magnetic field. The width of the region filled with material is 0.4 m and its geometry is determined by the geometry of the first wall. As in the case of a straight stellarator it is expected that the ferritic shell lowers the rotational transform of the vacuum field. The permeability is assumed to be homogeneous across the blanket region (μ = 1.3). The decrease of the rotational transform is displayed in the following figure.

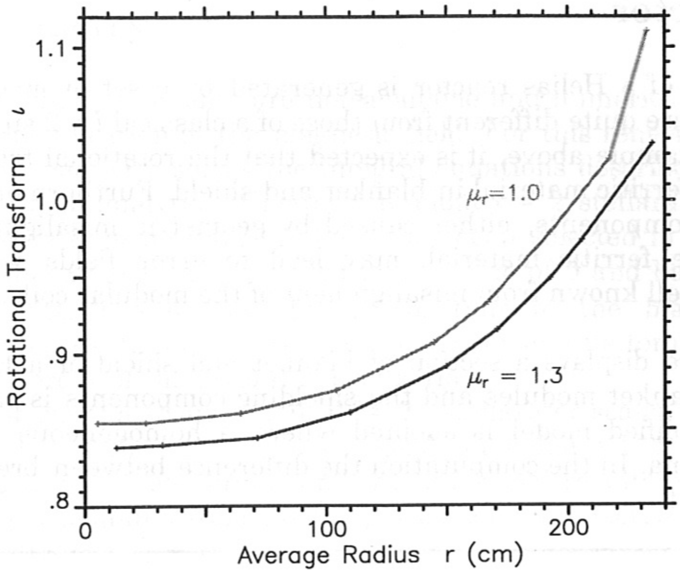

Fig. 6: Rotational transform in a vacuum field without ferritic blanket (μ_r = 1.0) and with ferritic blanket (μ_r = 1.3, lower curve)

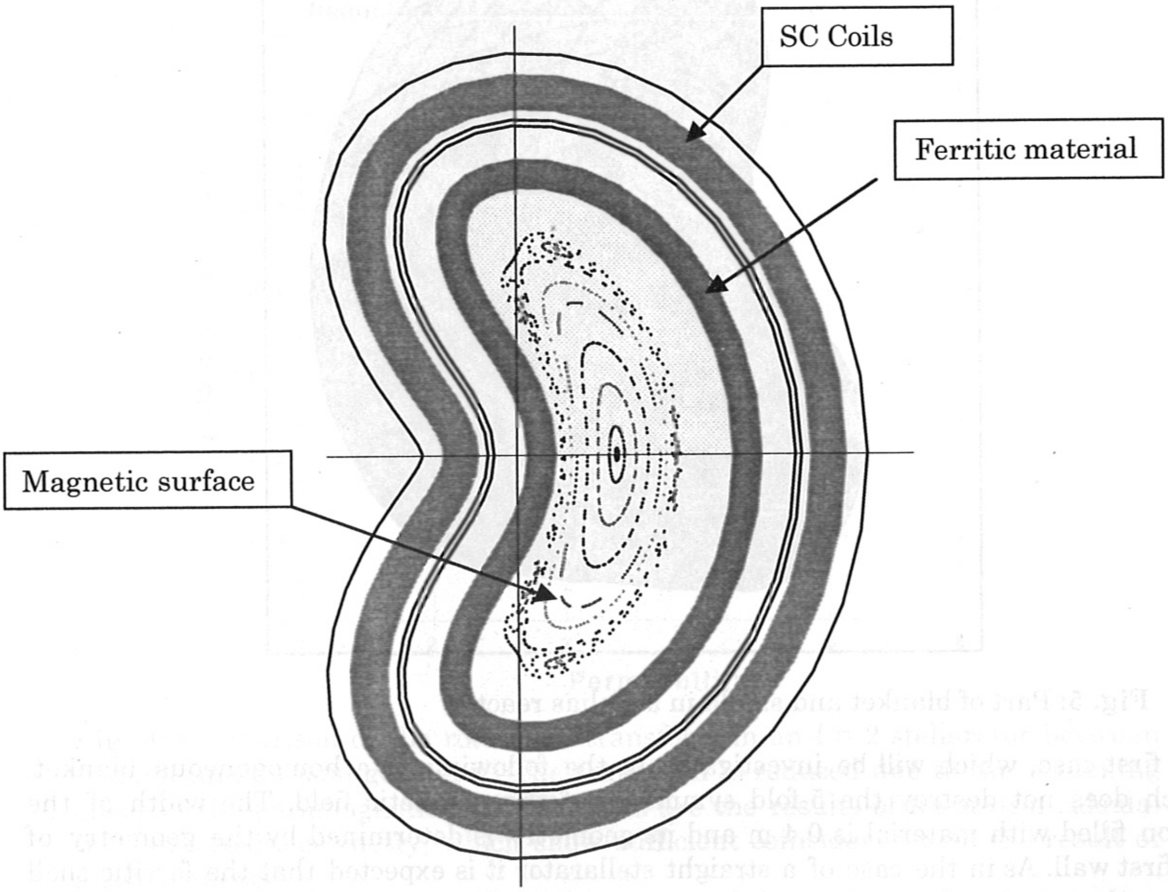

Fig. 7: Crossection of a Helias reactor at $\varphi = 0^{\circ}$. The region filled with ferritic steel is shown in grey color. The Poincaré plot is computed without any effect of the ferritic blanket. (μ_r = 1)

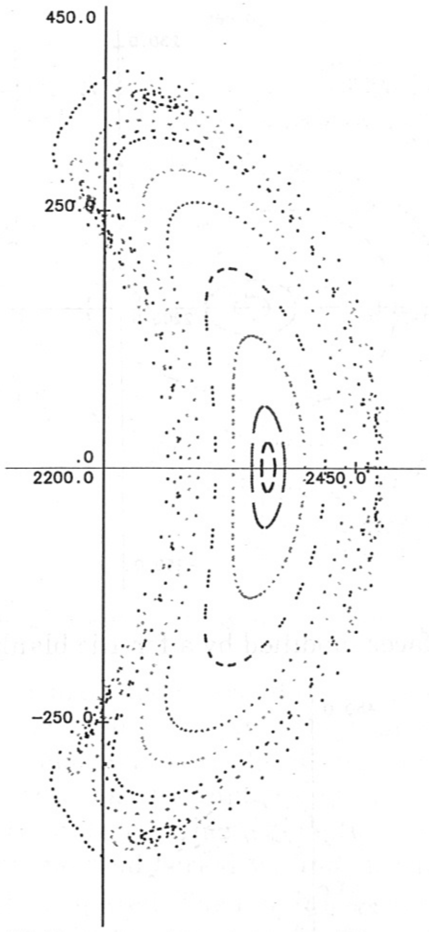

Fig. 8: Crossection of a Helias reactor at $\varphi = 0^o$. Magnetic surfaces modified by a ferritic blanket. ($\mu_r = 1.3$)

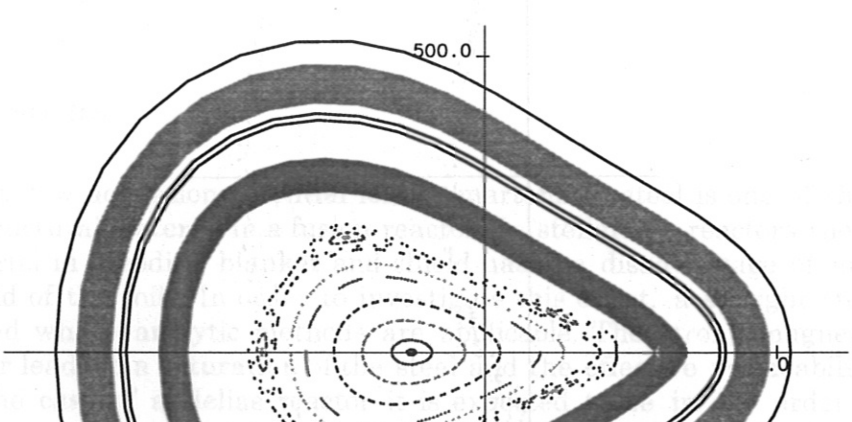

Fig. 9: Crossection of a Helias reactor at $\varphi = 36^o$. Vacuum field of coils

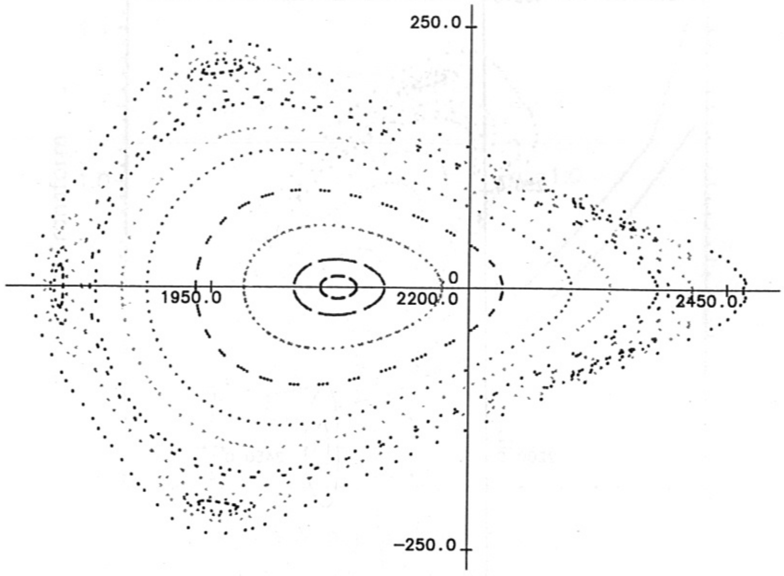

Fig. 10: Magnetic surfaces modified by a ferritic blanket. $\varphi = 36^{\circ}$. ($\mu_r = 1.3$)

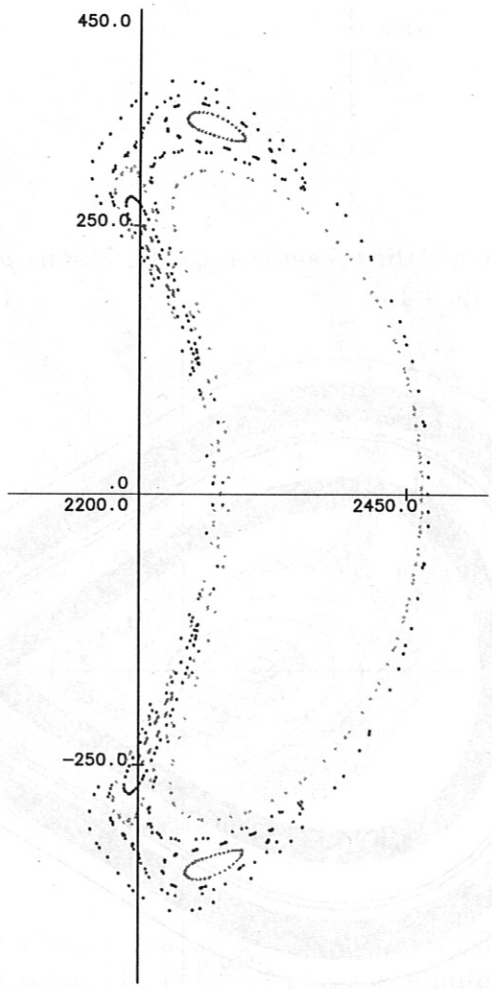

Fig. 11: Effect of ferritic blanket: $\mu = 1.3$, $\mu = 1$ in one period. $\varphi = 0^{\circ}$

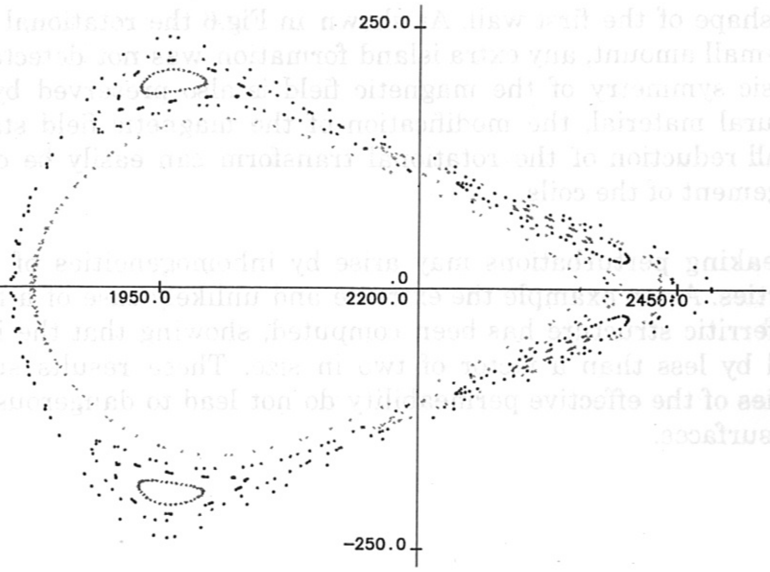

Fig. 12: Effect of ferritic blanket: $\mu = 1.3$, $\mu = 1$ in one period. $\varphi = 36^o$

Symmetry breaking field errors are particularly dangerous since resonance phenomena may lead to island formation. This effect requires high precision of the coil system and the toroidal arrangement of coils. Symmetry-breaking perturbations also occur if the structural components violate the basic symmetry of the magnetic field, which either arises from geometrical errors or from inhomogeneities of the ferritic steel. To study this effect the extreme case of one field period without ferritic material ($\mu = 1$) and four periods with $\mu = 1.3$ have been computed. The results are shown in Figs. 11 aqnd 12. The modification of the magnetic field in the inner region is small, mainly the islands at the boundary are increased by some amount.

6. Conclusions

Because of its low activation potential ferritic/martensitic steel is one of the main candidates as structural material in a fusion reactor. In stellarator reactors the presence of ferritic material in breeding blanket and shield has the disadvantage of modifying the magnetic field of the coils. In order to investigate this effect, a straight stellarator has been analysed where analytic methods are applicable. The strong magnetic field of a fusion reactor leads to a saturation of the steel and the effective permeability is smaller than 2. In the case of a Helias reactor it is expected to be in the order of 1.3. The effective permeability depends on the local magnetic field, however in the present computations it is assumed as a constant throughout the blanket region.

The model of a straight stellarator shows the expected reduction of the inner magnetic field and the reduction of the rotational transform. In case of $\mu = 2$ this can decrease the transform by 20%. The comparison with toroidal geometry shows that the analytic computaion of the straight stellarator is a good approximation to the toroidal stellarator.

In order to study the effect in a Helias reactor a homogeneous shell of 0.4 m width and an effective permeability of 1.3 has been modelled around the plasma. The geometry is given by the shape of the first wall. As shown in Fig.6 the rotational transform is only reduced by a small amount, any extra island formation was not detected (see Fig. 8 and 10). If the basic symmetry of the magnetic field is also preserved by the presence of ferritic structural material, the modification of the magnetic field stays at a tolerable level, the small reduction of the rotational transform can easily be compensated by a proper arrangement of the coils.

Symmetry-breaking perturbations may arise by inhomogeneities of the steel and its ferritic properties. As an example the extreme and unlikely case of a full period (one in five) without ferritic structure has been computed, showing that the islands at iota = 1 are perturbed by less than a factor of two in size. These results suggest that small inhomogeneities of the effective permeability do not lead to dangerous perturbations of the magnetic surfaces.